6.6 THE JUNE 8, 2005 TORNADIC BOW ECHO IN SOUTH DAKOTA

Ken Harding, Cory Behnke, Troy Kleffman, and Ryan Knutsvig
NOAA/NWS, Aberdeen, South Dakota

1. INTRODUCTION

On June 8, 2005, a bow echo developed and moved rapidly across central and northeastern South Dakota. Several anemometer readings exceeded 50 m s^{-1} during the most intense phase of this bow echo. As the bow echo reached maturity, numerous mesovortices formed along the leading edge. Several of theses mesovortices were tornadic, producing damage rated up to F-1. This paper will review the synoptic and mesoscale settings for this event and focus on the transition from a damaging straight line wind event to the tornadic phase. A detailed storm survey was conducted that correlated the most intense surface damage with the tracks of the mesovortices along the leading edge of convection.

2. PRE-STORM ENVIRONMENT

The June 8, 2006 00:00 UTC (hereafter, all times are in UTC) 300 mb analysis showed a broad trough of gepotential heights over the western United States with a 40+ m s^{-1} wind maximum moving through the base of the trough(Fig 1). This trough and associated wind maximum allowed for upper diffluence over the western Dakotas and an area of divergence associated with the left exit region of the wind maximum.

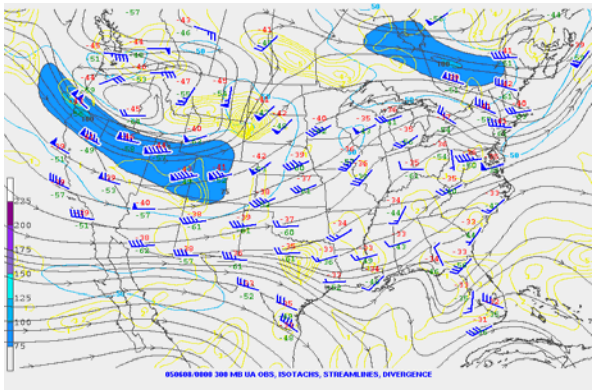

Figure 1: 300 mb analysis for 0000 UTC 8 June 2005. Blue isolines are isotachs (knots), streamlines are gray, and divergence is yellow.

At 850 mb (Fig.2), a broad area of low heights existed along the front range of the Rocky Mountains. Southerly winds of 10 – 15 m s^{-1} exist from northern Texas through central Nebraska. An axis of high dewpoints greater than 17°C was aligned within the area of the highest winds. At 500 mb (not shown), a closed low was analyzed over western Oregon with a vorticity maximum moving across central Wyoming.

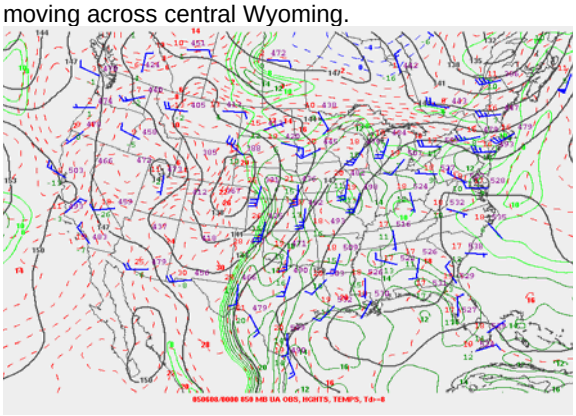

Figure 2: 850 mb analysis for 0000 UTC 8 June 2005. Isolines of geopotential heights are in black (decameters), dewpoints are in green (°C)

The RUC surface analysis (not shown) revealed an area of surface low pressure along the central Nebraska-South Dakota border. An inverted surface trough of low pressure was evident in central South Dakota with an area of easterly surface winds east of this feature. Figure 3 shows surface-based convective available potential energy (CAPE) in excess of 2000 J kg^{-1}. Convective inhibition (CIN) was 100 J kg^{-1} or less across the central and southern portions of South Dakota. At this time severe convection was ongoing in southwestern South Dakota. This pre-storm environment is similar to the dynamic pattern identified by Johns and Hirt (1987).

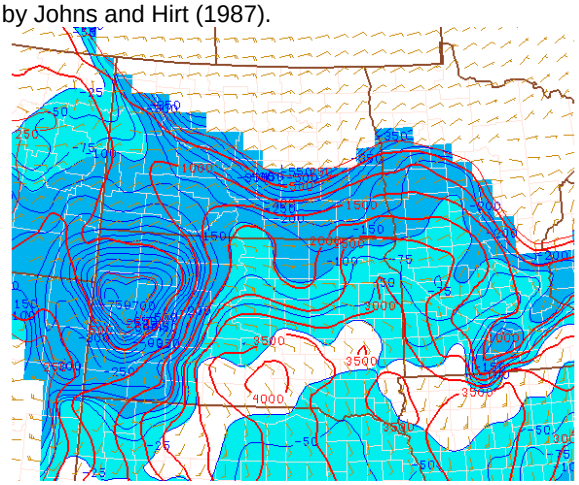

Figure 3: 0000 UTC 8 June 2006 RUC surface-based CAPE (red lines) and CIN (blue shading) in J kg^{-1}.

Corresponding author address: Ken Harding, National Weather Service, 824 Brown County 14 South, Aberdeen, SD 57401; e-mail: kenneth.harding@noaa.gov

The exception is the relatively weak 500 mb winds and atypical formation of the thunderstorms along an inverted surface trough vice a cold frontal boundary.

3. CELL MERGER TO BOW ECHO EVOLUTION

Figure 4 shows a 0.5 degree base reflectivity image from the KUDX WSR-88D at 00:43 June 8 (hereafter, all dates are June 8, 2005). An isolated supercell thunderstorm is located just ahead of the main convective line in south central South Dakota. This supercell produced tornadoes in Jackson County prior to this time. The line overtakes the cell and ingests it by 0143 UTC (image not shown). The first report of damaging surface winds was received at the time of cell merger with the linear convection. A cooperative observer in Hayes (central Jones County) measured a wind gust of 43 m s^{-1} at 0144 UTC. As the cell merger continued, the linear convection began to take on a bowing shape, consistent with the Klimowski et al. (2004) observation that 45% of squall lines in their study quickly transitioned to a bow echo after a cell merger. The cell merger was complete by 0204 UTC as the supercell was no longer discernable in the reflectivity data (Fig. 5), and the mesocyclone was losing definition as noted in the storm relative velocity (SRM) data (not shown). As the bow echo continued to evolve, a well-defined rear inflow jet (RIJ) formed (Rutunno et al., 1988 and Weisman, 1992).

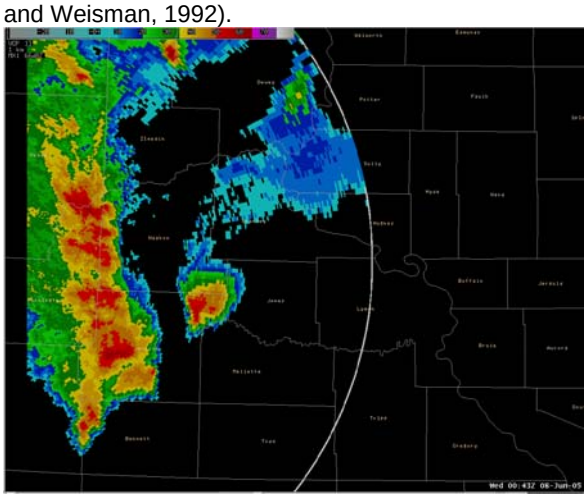

Figure 4: WSR-88D base reflectivity image from KUDX at 0043 UTC June 8 2005.

A RIJ is often associated with damaging surface winds in an area behind the leading edge of convection. Weisman (1992) showed that the area affected by the descending RIJ was directly related to the strength of the unidirectional wind shear below 2.5 km (and with a moderate environmental CAPE). His results indicated a broad area of descending RIJ winds with shear values

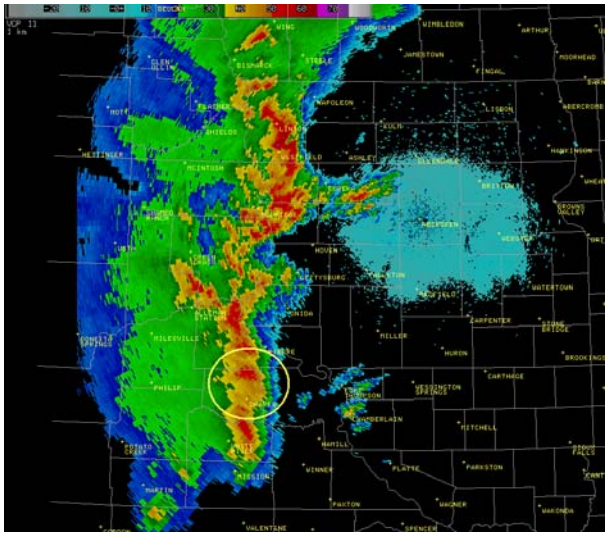

Figure 5: 0204 UTC KABR WSR-88D base reflectivity. Area of previous cell merger is indicated by yellow circle.

10 to 15 m s^{-1}. When the shear was increased to greater than 20 m s^{-1}, the RIJ tended to stay elevated 2-3 km above the ground with a smaller branch of the RIJ reaching the surface directly behind the gust front. Even though smaller in aerial extent, the stronger shear case had more intense surface winds. By 0238 UTC, the bowing segment is evident in both reflectivity data and the base velocity data in figures 6 and 7.

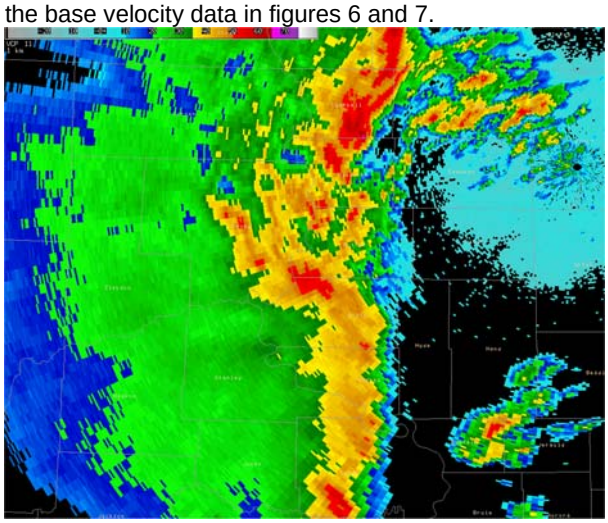

Figure 6. 0238 UTC KABR WSR-88D base reflectivity.

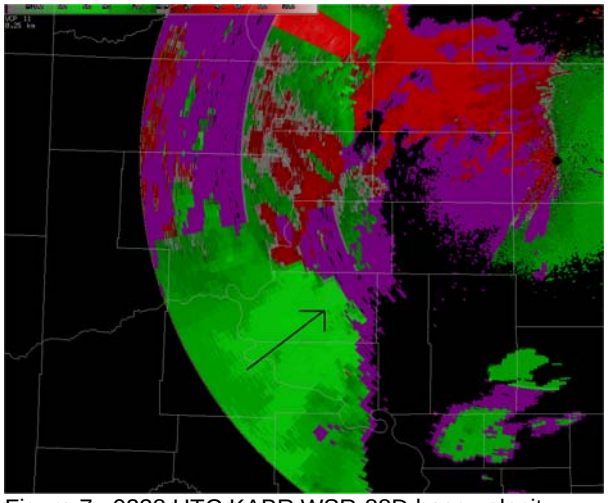

Figure 7. 0238 UTC KABR WSR-88D base velocity. Arrow points along the axis of greatest ground relative winds with values in excess of 35 m s^{-1}.

4. MESOVORTEX EVOLUTION

Squall lines and bow echoes fall into the general category of quasi-linear convective systems (QLCSs). Weisman and Trapp (2003) point out "…Recent observations suggest that many of the severe weather events associated with QLCSs, including both tornadoes and damaging straight-line winds, are associated in some way with the development of significant low-level meso-γ-scale (e.g., 2-40 km) vortices within such systems". The strength of these mesovortices in their simulations was dependent on the environmental shear. When the unidirectional wind shear exceeded 20 m s^{-1}, low level mesovortices were able to persist for as long as several hours and were associated with a larger area of potentially damaging winds at the surface (Trapp and Weisman, 2003). The origin of these mesovortices was suggested to be caused by a cyclonic-anticyclonic couplet around a downdraft in the leading edge of the precipitation. Recent examination of airborne DOPPLER radar data from the 5 July 2003 BAMEX bow echo has led Wakimoto et al. (2006) to propose a different mechanism for the formation of these leading edge mesovortices. Figure 8 suggests the proposed mechanism isn't a downdraft associated within the precipitation but a mechanically driven downdraft forced by the pressure gradient force arising due to continuity constraints in the presence of buoyant parcels. The couplet that forms along the leading edge of the cold pool more closely matches observations from BAMEX and does not require a raining downdraft.

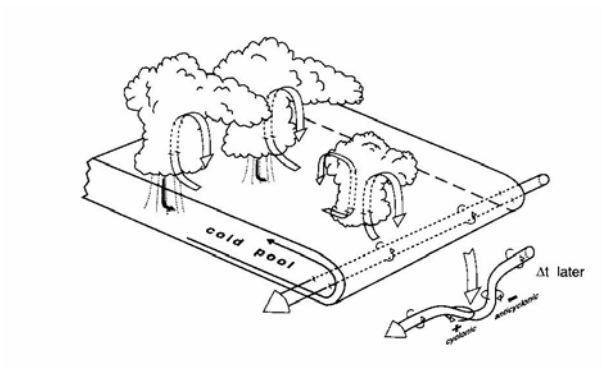

Figure 8. Mechanically driven downdraft forced by continuity constraints due to parcel buoyancy in an area void of precipitation (Wakimoto et al. 2006)

The Trapp and Weisman (2003) modeling study produced areas of intense winds as strong as or stronger than the RIJ induced surface winds near mesovortices. The area and duration of the mesovortex winds were an order of magnitude larger than the RIJ-induced surface winds for the same modeled QLCS. These results suggest the intense swaths of damage contained within the overall bow echo damage area are not the result of RIJ winds reaching the surface. Figure 9 from Trapp and Weisman (2003) shows an idealized illustration of the difference in the areas affected by the most intense winds in their simulations. Well documented damage surveys from QLCS storms observed during the Bow Echo and Mesoscale Convective Vortex Experiment (BAMEX) confirm the primary straight line wind damage was not collocated with the apex of the bowing segments but instead was along tracks of radar identified mesovortices (Atkins et al, 2005). In another study, Atkins et al. (2004) studied 13 mesovortices in a squall line that moved across Iowa and Missouri. Their results showed that 7 of the mesovortices became tornadic, producing damage up to F1 intensity. In this case, Atkins et al. noted the tornadic phase was initiated only after the transition to a bow echo was ongoing. Earlier studies by Forbes and Wakimoto (1983) documented the potential for numerous tornadoes produced by bow echoes. Indeed in this case presented here, at least 6 separate tornadoes were produced in the direct vicinity of pre-existing mesovortices after the QLCS began to bow out. The reader is again referred to Figure 6 where the QLCS is beginning the transition towards a bow echo. Several 'notches' in the reflectivity are evident with the main one being along the apex of the forming bow. This notch had a cyclonic circulation associated with it and continued to grow upscale, eventually becoming the north end 'bookend' vortex. Several smaller

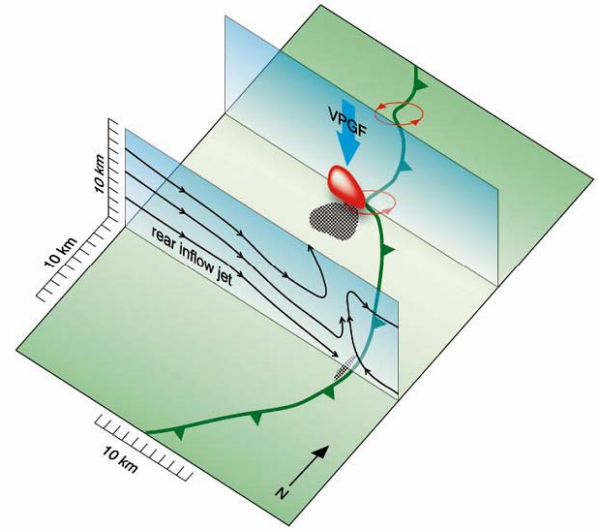

Figure 9: Schematic of area affected by damaging surface winds (hatched black). From Trapp and Weisman (2003).

mesovortices were evident in the reflectivity data by 0258 UTC (Fig. 10). These mesovortices formed over a period of one or two volume scans (5 to 10 minutes). Mesovortex 1 in the figure would go on to produce a F1 tornado in 15 minutes. The other arrow indicates another mesovortex that would rotate back into the northern bookend vortex.

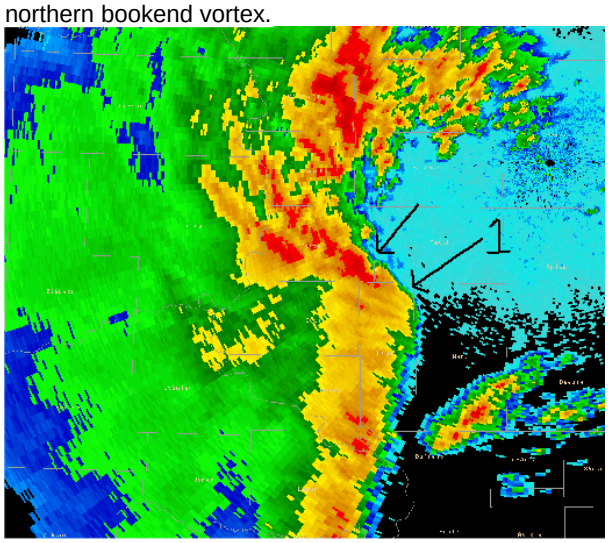

Figure 10: Base reflectivity at 0258 UTC from the KABR WSR-88D. The one refers to the incipient mesovortex that would produce the first tornado.

5. THE TORNADIC PHASE

After the 0258 UTC volume scan, several more mesovortices formed. Atkins et al. (2005) noted "All the tornadic vortices formed coincident with or after the genesis time of the rear inflow jet" While vertical cross sections of this case's RIJ have not been completed, the continued acceleration of the leading edge of the bow suggests that the RIJ is becoming better defined and reaching the surface. Indeed, wind reports from the vicinity of the apex of the bow continued to exceed 30 m s^{-1} through this time. Figure 11 shows the evolution by 0342 UTC. Three distinct mesovortices are indicated by the black lines on the figure. The southernmost vortex will go on to produce 2 tornadoes while the northern one produced 3 tornadoes. Figure 12 is the 0.5 degree storm relative motion (SRM) image taken at the same time. All three mesovortices are evident. Although other mesovortices formed over the next two hours, these were the most prolific tornado producers.

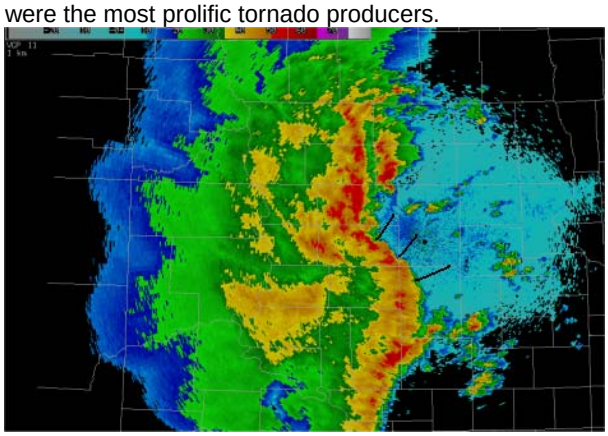

Figure 11: 0342 UTC KABR WSR-88D 0.5 degree reflectivity. Mesovortices are indicated by black lines.

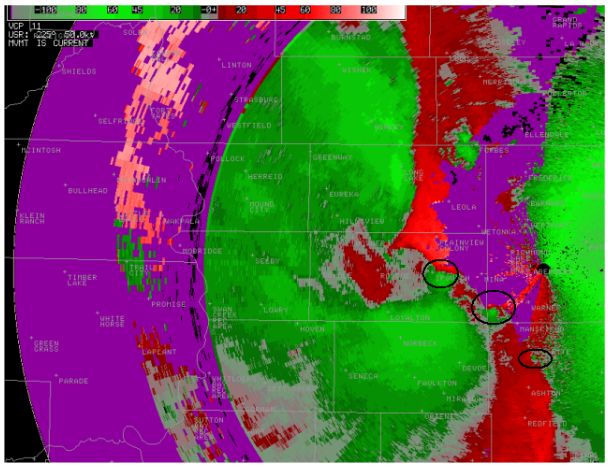

Figure 12: As in figure 13 except SRM.

The Atkins et al. (2004, 2005) studies of two bow echoes presented detailed vertical and temporal evolution of several mesovortices. They found the mesovortices that produced tornadoes had at least double the lifespan and stronger V_r shear than non-tornadic mesovortices (V_r definition is in figure 13). In a finding that may help the warning forecaster, they showed the pre-tornadic mesovortices had stronger V_r shear well before producing tornadoes. They found no correlation between diameter and tornadic potential. In the case presented here, mesovortex one (from figure 10, and again as the middle one from figure 11) is examined. Figure 13 shows the time evolution of V_r shear.

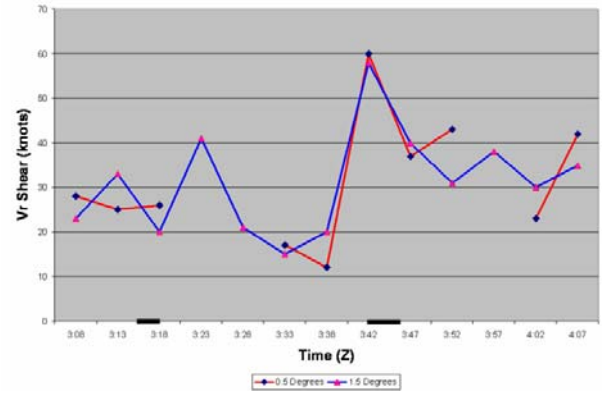

Figure 13: V_r shear (defined as $(V_{max} - V_{min})/2$, where V_{max} and V_{min} are the outbound and inbound mesovortex velocity maximum, respectively). Red line is 0.5 deg. And blue line is 1.5 deg. Elevation. Tornado time is indicated by heavy black line on time axis.

Compared to the non-tornadic mesovortices (not shown), this circulation was initially strong and lasted well over an hour, producing two tornadoes. These preliminary results agree well with the Atkins et al. studies (2004, 2005). Figure 14 is a 0.5 degree base reflectivity image zoomed in on this mesovortex at the approximate time of the first tornado. Although a hook-like echo is present in the reflectivity data, Weisman

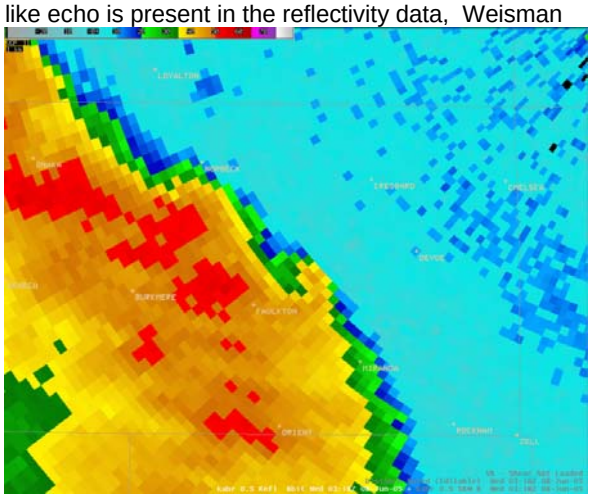

Figure 14. 0318 UTC 0.5 deg. Base reflectivity from the KABR WSR-88D.

And Trapp (2003) point out these low level circulations are not like supercell mesocyclones in that they do not have a persistent, rotating updraft and do not move deviant from the mean wind. Thus, this 'hook' in the reflectivity data should not be confused with the similar structure seen in classical supercells. As in many cases of squall lines and bow echoes, the SRM velocity data can be difficult to interpret due, in part, to velocity dealiasing and range unfolding difficulties. Figure 13 shows such a case. Although cyclonic rotation is evident, it is not as strong or compact as radar operators are used to seeing in classical tornadic depictions. Thus, the radar operator must be aware of the implications of the reflectivity notches and hook-like structures and interpret them in the context of the QLCS environment and examine them for time continuity and V_r shear strength.

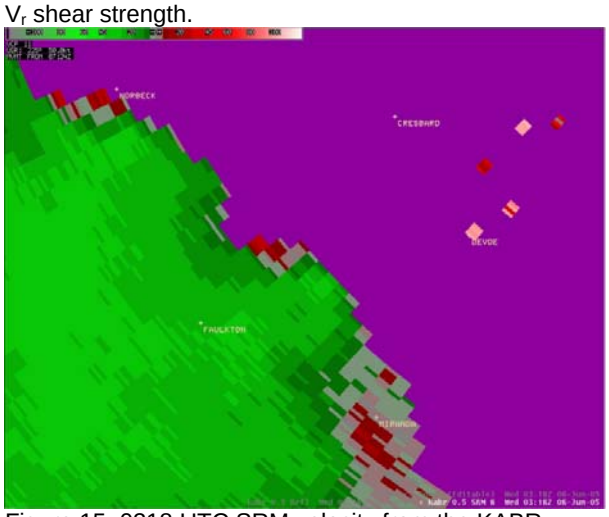

Figure 15. 0318 UTC SRM velocity from the KABR WSR-88D.

More detailed examination of each mesovortex is ongoing by the authors.

6. DAMAGE SURVEY AND CONCLUSIONS

Of other interest in this case was the strength of the surface winds in the vicinity of the RIJ. Numerous gauge readings in excess of 45 m s^{-1} and damage surveys confirming damage consistent with these wind speeds were documented from the time of the first cell merger to just before the time when tornadic production peaked. After the tornadic phase was over, no reports of surface winds exceeding 35 m s^{-1} were received. This bow echo produced a large area of damage and six tornadoes. NWS warning meteorologists are encouraged to actively monitor these mesovortices and monitor their evolution to better warn people in the path of these storms. Careful attention to radar-derived velocities (SRM calculations) is needed as individual mesovortices are much better visualized with the correct mesovortex motion which can be significantly different than the motion of the larger bow echo.

The reader is referred to the following web page for radar animations, damage survey information, and damage photographs:

http://weather.gov/aberdeen/june8storm

7. REFERENCES

Atkins, Nolan T., J. M. Arnott, R.W. Przybylinski, R.A. Wolf, and B. D. Ketcham, 2004: Vortex Structure and Evolution within Bow Echoes. Part I: Single-Doppler and Damage Analysis of the 29 June 1998 Derecho. *Mon. Wea. Rev.*, **132**, 2224-2242.

_____, C. S. Bouchard, R. W. Przybylinski, R. J. Trapp, and G. Schmocker, 2005: Damaging Surface Wind Mechanisms within the 10 June 2003 Saint Louis Bow Echo during BAMEX. *Mon. Wea. Rev*., **133**, 2275-2296.

Forbes, G., S., and R. M. Wakimoto, 1983: A concentrated outbreak of tornadoes, downbursts, and microbursts, and implications regarding vortex classification. *Mon. Wea. Rev.,* **111,** 220-235.

Johns, R. H., and W. D. Hirt, 1987: Derechos: Widespread convectively induced windstorms. *Wea. Forecasting*, **2**, 32-49.

Klimowski, B. A., M. R. Hjelmfelt, and M. J. Bunkers, 2004: Radar observations of the early evolution of bow echoes. *Wea. Forecasting*, **19**, 727-734.

Trapp, R. J., and M. L. Weisman, 2003: Low Level Mesovortices within Squall Lines and Bow Echoes. Part II: Their Genesis and Implications. *Mon. Wea. Rev*., **131**, 2804-2823.

Wakimoto, R. M., Murphey, H. V., Nester, A., Jorgensen, D. P., and Atkins, N. T., 2006: High Winds Generated by Bow Echoes. Part I: Overview of the Omaha bow Echo 5 July 2003 Storm during BAMEX. Submitted for Publication in *Mon. Wea. Rev.*

_____, _____, Davis, C. A., and Atkins, N. T., 2006: High Winds Generated by Bow Echoes. Part II: The Relationship between Mesovortices and Damaging Straight-Line Winds. Submitted for Publication in *Mon. Wea. Rev.*

Weisman, M. L., 1992: The role of convectively generated rear-inflow jets in the evolution of long-lived mesoconvective systems. *J. Atmos. Sci.,* **49,** 1826-1847.

_____, 1993: The genesis of severe, long-lived bow echoes. *J. Atmos. Sci.,* **50,** 645-670.

_____, and R. J. Trapp, 2003: Low Level Mesovortices within Squall Lines and Bow Echoes. Part I: Overview and Dependence on Environmental Shear. *Mon. Wea. Rev*., **131**, 2779-2803.